Atmospheric and Oceanic Data Assimilation Plus ENsembles Generation (AODA-PENG)

A. Hense (1), J. Baehr (2), J.S. von Storch (3), W.A. Müller (3), A. Bott (1), V. Romanova (1),
S. Brune (2), M. Zeller (2), J. Kröger (3), M. Kaleem (1), K. Kulkarni (3), H. Pohlmann (3), L. Nerger (4)

(1) Meteorologisches Institut, Universität Bonn (3) Max-Planck-Institut für Meteorologie
(2) Institut für Meereskunde, Universität Hamburg (4) Alfred Wegener Institute for Polar and Marine Research, Bremerhaven

The Project AODA-PENG aimed to provide improvements to the MiKlip prediction system in three ways: (i) we implemented and tested state-of-the-art ensemble generation techniques in the prediction system based upon MPI-ESM-LR, (ii) we applied EnKF data assimilation to the oceanic component of MPI-ESM-LR, and (iii) we analyzed the aerosol forcing as a potentially important external forcing factor.

Assimilation of oceanic observations with the ensemble Kalman Filter

Sebastian Brune, M. Zeller, J.Baehr, L.Nerger, H. Pohlmann, K. Kulkarni, W.A. Müller

Initialization of MPI-ESM-LR decadal hindcasts with coupled assimilation of oceanic observations and atmospheric re-analysis data 1958-2014:

- Oceanic assimilation of monthly EN4 observations with the singular evolutive interpolated ensemble Kalman filter from the Parallel Data Assimilation Framework (PDAF, http://pdaf.awi.de).
- Atmospheric nudging of monthly ERA40/ERAInterim reanalysis.

Assimilation:

- Globally high correlation with 2m Temp, regionally high correlation with heat content,
- High correlation with AMOC at 26°N.

Hindcasts:

- Globally high correlation with 2m temperature for lead years 1 (not shown) and 2-5 (Fig.1), except for the Pacific Ocean.
- Improved skill for AMOC and AMOC-Ekman at 26°N for up to 5 lead years (Fig.2) when compared to climatology.

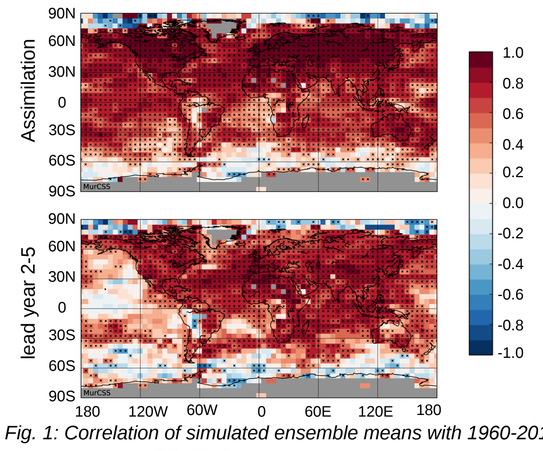

Fig. 1: Correlation of simulated ensemble means with 1960-2014 yearly mean HadCRUT4 2m temperature observations: coupled assimilation run (above) and lead years 2 to 5 of the hindcasts initialized by the coupled assimilation (below).

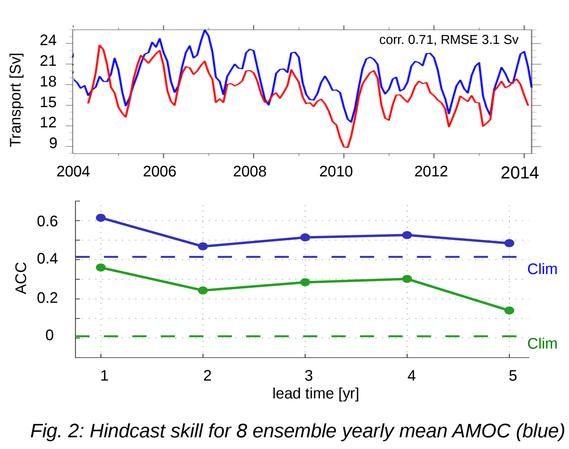

Fig. 2: Hindcast skill for 8 ensemble yearly mean AMOC (blue) and AMOC minus Ekman-Transport (green). Corresponding skill of a repeated seasonal cycle (climatology) is indicated with dashed lines.

Hindcast initialization using area selective nudging of oceanic reanalyses

Jürgen Kröger, J.S.von Storch

In conventional full area nudging to oceanic reanalyses the imprint of the reanalysis model to MPI-ESM-LR may have negative impact on the prediction skill.

- Applying the state estimates only in regions where the estimates are better constrained by real observations may lead to better skill.
- Area selective nudging towards T & S from ocean reanalysis GECCO2 based on a mask that reflects real ocean data coverage in 2008 EN3 data (Fig. 3).
- Multi-year AMOC hindcasts with reduced area initialization outperform those with full area initialization in large parts of the Atlantic basin (Fig. 4), elsewhere they are comparable.

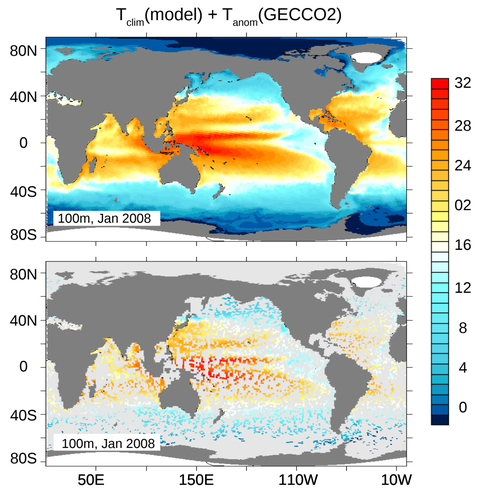

Fig. 3: Temperature data at the 100m level used for full area nudging (above) and area selective nudging (below).

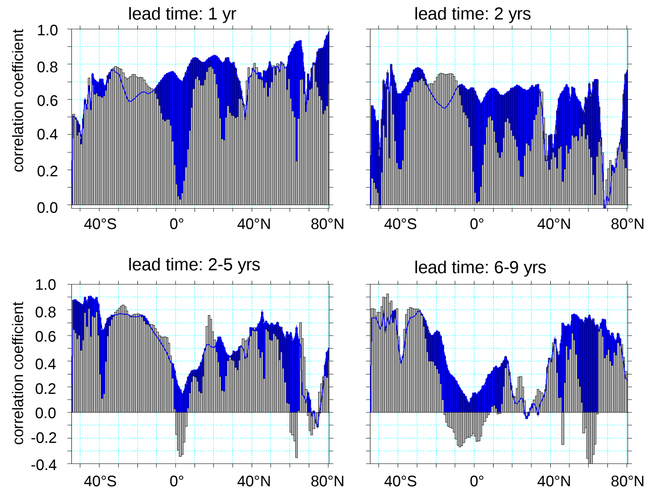

Fig. 4: Correlation w.r.t assimilations of ensemble mean annual (top) or multi-annual (bottom) mean AMOC at 1000 m: hindcasts with full area (gray) and area selective (blue) initialization.

Ensemble generation using oceanic breeding

Vanya Romanova, A. Hense

Provide bred vectors for ensemble generation in decadal prediction,

- Bred a-priori random noise over time,
- Extract fastest growing errors,
- Consider only the slowest modes of the ocean physical processes,
- Determine local BV around an almost fixed in time oceanic state.
- Implementation in MPI-ESM T31L31/GR30L40
- Perturbations in oceanic temperature, salinity, meridional, zonal velocity

Metric: weighted total energy as sum of kinetic and available potential energy:

$$\|Z_f\|_{end} = \frac{w_u}{2}\int u'^2 dV + \frac{w_v}{2}\int v'^2 dV + \frac{w_\rho g}{2\rho_0}\int \frac{\rho'^2}{\rho_z} dV$$

Rescaling: ratio between the total energy growth at the first and the final state:

$$C = \sqrt{\frac{\|Z_f\|_{initial}}{\|Z_f\|_{final}}}$$

- Calculated nine BV using 12 months looping period over 10 iterative steps. Areas with strongest total energy growth shown on Fig. 5
- Demonstrated increased spread along the integration time (Fig. 6).

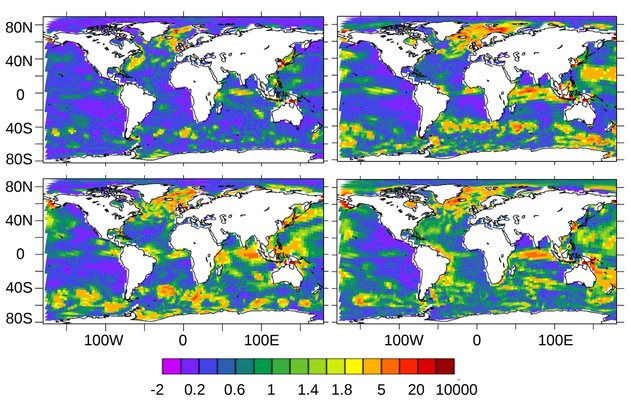

Fig. 5: Spatial pattern of ensemble mean perturbation growth rate (averaged with depth) at final iteration for four out of eight Bred Vectors. The unit is dimensionless.

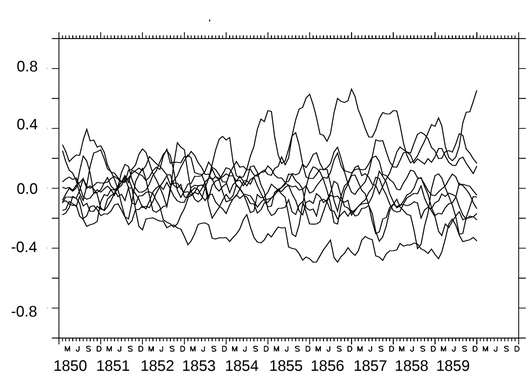

Fig. 6: Time series of surface temperature anomalies of ensemble initialized with nine Bred Vectors.

Aerosols induced variability for the Atmospheric Radiative Energy Balance

Muhammad Kaleem, A. Hense, A. Bott

Importance of aerosols to the atmospheric radiative energy balance (AREB) on interannual to decadal time scales

Simulations with ECHAM6-HAM:

- HAM-dir (direct): interactive aerosol dynamics determining the radiative properties like aerosol optical depth and scattering effects
- HAM-full (direct + indirect): interactive aerosol dynamics determining the radiative properties and cloud properties like droplet or ice crystal concentration
- Aerosol induced variability (determined by two-way ANOVA) is largely significant over tropical and sub-tropical regions (Fig. 7) ~ 80% for these two cases (HAM-full, HAM-dir)
- HAM-dir is more sensitive than HAM-full
- SST induced variability is not significant for both cases
- In the hindcast of the tropical AREB there is a significant aerosols climatic effect over the 5 to 10 years time scale.

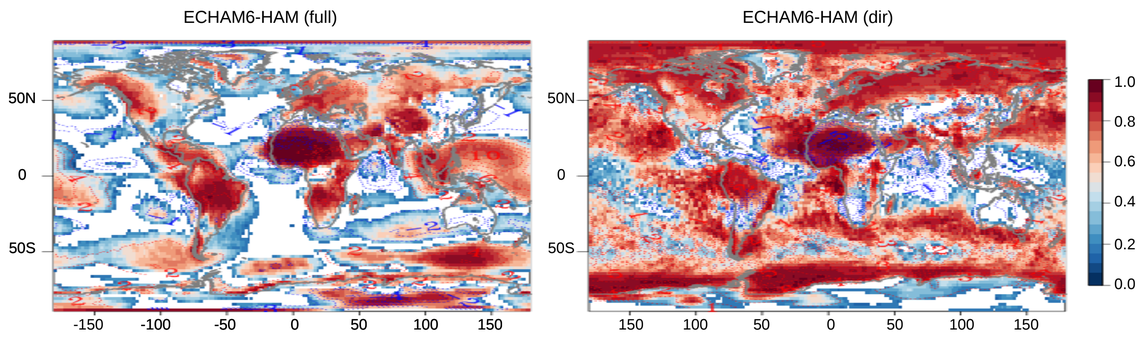

Fig. 7: Two way ANOVA, relative contribution of aerosol effects to total variance of atmospheric radiative energy balance annual mean 1995-2004 for HAM-full (left) and HAM-dir (right), significant at 5% level, contour plot is based on plain difference. Positive values of the contours in these plots indicate the reduction in radiative loss and gain of static stability and negative values show an increment in radiative loss and less static stable atmosphere

Coupled assimilation of sub-surface oceanic observations using the EnKF and atmospheric observations using nudging leads to hindcast skill which is improved in terms of both temperature and AMOC correlation when compared to the free model. When sub-surface oceanic reanalysis data are nudged into the oceanic part of MPI-ESM-LR, AMOC skill is improved when hindcasts are initialized using the area selective method when compared to full area nudging. The breeding technique for creating geographically localized ocean disturbances provide reasonable spread in a low resolution model set up and is a compatible candidate for further implementation in the prediction system. On decadal time scales the climatic effect of aerosols on the tropical Atmospheric Radiative Energy Balance is significant, therefore they should be included in a decadal prediction system.

The MiKlip project AODA-PENG was supported by the German Ministry of Education and Research (BMBF) under grant 01LP1157C.
We thank the German Climate Computing Centre (DKRZ) for providing the computing resources for our simulations under project bu0801.